# Velocity of Sound at 1 MHz Near the $He^4$ Critical Point

R. C. Williamson
*Center for Materials Science and Engineering, Massachusetts Institute of Technology, and NASA Electronics Research Center, Cambridge, Massachusetts*

and

C. E. Chase
*Francis Bitter National Magnet Laboratory,* Massachusetts Institute of Technology, Cambridge, Massachusetts*

(Received 27 June 1968)

The velocity of 1-MHz sound waves has been measured in $He^4$ along several isotherms just above the critical temperature. The results indicate that along the critical isotherm, the quantity $\rho/u^2$ diverges approximately logarithmically as a function of $|P-P_c|$. Such a singularity at the critical point is to be expected in view of the corresponding singularity in $C_v$. Additional velocity measurements were made in the saturated liquid, along isotherms several tenths of a degree above $T_c$, and along the 4.5 and 5.0°K isotherms in the liquid. The specific-heat ratio has been calculated along the latter two isotherms and along the critical isotherm.

## I. INTRODUCTION

In recent years, interest in studies in critical points has been reawakened largely because of the discovery of an approximately logarithmic singularity in the specific heat at constant volume $C_v$ at the critical point in argon,[1] oxygen,[2] and helium.[3] These results have necessitated a reexamination of much of the past experimental work on critical points, which is apparently contradictory, and a reformulation of the theories of the critical region. One implication of the singularity in $C_v$ is that a corresponding singularity should occur in the adiabatic compressibility and that the sound velocity $u$ (in the absence of dispersion) should go to zero as the critical point is approached.[4,5] The purpose of this experiment was to search for such a singularity.

There have been many measurements of sound velocity near the critical point in various substances,[6–14] all of which appear to show only a finite velocity minimum. However, closer examination of these results shows that, because of the limited resolution of the measurements, they are not inconsistent with a weak singularity in the adiabatic compressibility $\kappa_S = 1/\rho u^2$ at the critical point.

We have measured the sound velocity in the region of the critical point of $He^4$ with improved resolution, and find convincing evidence for the existence of the expected singularity. Measurements were made in the liquid along the vapor-pressure curve, along a series of closely spaced isotherms in the vicinity of the critical temperature, and along several isotherms at temperatures a few tenths of a degree above and below $T_c$. In addition to yielding information about the nature of the critical-point singularities, these measurements enable us to evaluate the specific-heat ratio $\gamma$ at several temperatures and pressures where values of the isothermal compressibility are known. Some preliminary results of this work have previously been reported.[5,15,16]

## II. EXPERIMENTAL METHOD

### 2.1 Brief Description

Measurements of the sound velocity at 1 MHz were made using a high-resolution, phase-sensitive method. The ultrasonic etalon was contained in a vacuum-jacketed can immersed in a bath of liquid helium. Temperature was measured and controlled within $\pm 10^{-4}$ °K by a carbon resistance thermometer and heater connected to an automatic temperature controller.[17] Pressure was measured by a Wallace-Tiernan gauge and a mercury manometer.

### 2.2 Cryostat Design

The experimental apparatus is shown in Fig. 1. The sample space consisted of a 9-cm-long, heavy-walled copper can (1) within which the pressure and temperature of the sample of helium were regulated. The high-conductivity copper aided the maintenance of a uniform temperature throughout the can and within the enclosed fluid. This can was surrounded by a brass can (2) to provide a vacuum or exchange-gas space. The entire apparatus was immersed in a liquid-helium bath which was normally held at 4.2°K.

A stainless-steel tube (4), (to be referred to as the pressure tube), ran from the inner can up to the top of the cryostat through the center of the exchange-gas pumping line. This arrangement helped to insulate the pressure tube from the helium bath and to maintain a uniform temperature gradient along the pressure tube from the top of the inner can to the top of the cryostat, thus preventing condensation along the tube and avoiding unstable temperature distributions and erroneous pressure readings.

At the beginning of each run, the inner can was filled from the bath through the needle valve (5). Subsequent changes in density within the inner can were made by adding or removing fluid through

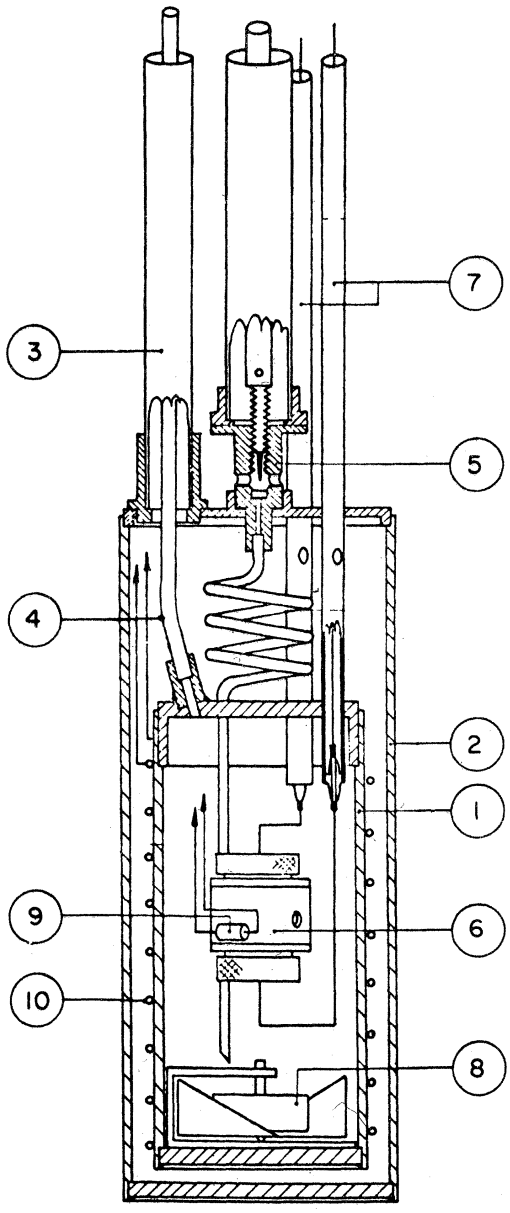


FIG. 1. Cryostat lower end. (1) copper inner can, (2) outer can, (3) exchange gas pumping line, (4) pressure tube, (5) filler valve, (6) ultrasonic etalon, (7) coaxial leads, (8) stirrer, (9) carbon resistor, (10) heater.

the pressure tube.

The sound etalon (6) was supported by the filler tube and located approximately in the center of the inner can. Within the etalon, two 1-cm-diam. X-cut quartz transducers were held accurately parallel with their faces horizontal in brass holders separated by a brass tube. Two stainless-steel tubes (7) supported the inner can and served as coaxial leads to the sound etalon.

A magnetic stirrer (8) within the inner can was provided to promote thermal equilibrium. The stirrer was driven by a permanent magnet located directly below the cryostat and rotated at 60 rpm by a motor.

### 2.3 Ultrasonic System

Details of the phase-sensitive detection system shown in Fig. 2 have been given previously.[18] The output of a 1-MHz crystal-controlled oscillator is fed through a gated amplifier to provide a pulse of amplitude $\approx$10 V and length 20 $\mu$ sec which excites the transmitting crystal. The received signal is amplified and compared (in the phase detector) with a reference signal derived from the oscillator. By means of the 1-$\mu$ sec variable delay, the phase of the reference signal can be shifted to maintain a constant phase relation with the received signal ("a null") as the ultrasonic delay changes. Changes in delay line setting are thus equal to changes in delay of the ultrasonic signal. Whitney and Chase[19] have thoroughly discussed the experimental method and the errors associated with this technique. Here we will discuss only our modifications of their apparatus and the errors peculiar to this research.

The choice of operating frequency was governed by two opposing considerations: Attenuation and dispersion become smaller as the frequency decreases, but at the same time it is necessary to increase the path length and errors due to gravitational effects are increased. We feel that our choice of 1 MHz represents a reasonable compromise that approximately minimizes the over-all errors due to these two effects.

In all runs, we used a path length of 0.3961 $\pm$0.0005 cm (corrected by 0.39% for the contraction of brass to helium temperature). Changes in path length over the temperature range of these measurements are negligible. This relatively short path was chosen at the sacrifice of velocity resolution to minimize the above-mentioned gravitational effects and because high attenuation was anticipated near the critical point.[8, 11, 14]

Errors due to spurious phase shifts and time delays in the circuitry were quite small. By adjusting the gain of the receiver amplifier to provide a nearly constant, optimum input to the 6BN6 mixer, delay errors were held to within $\pm$3 nsec. Changes in signal delays in the remainder of the electronics and in phase shift in the quartz transducers were negligible.

One major source of error in measurements of changes in ultrasonic delay was nonlinearities in the delay line, i.e., the dial reading of the delay

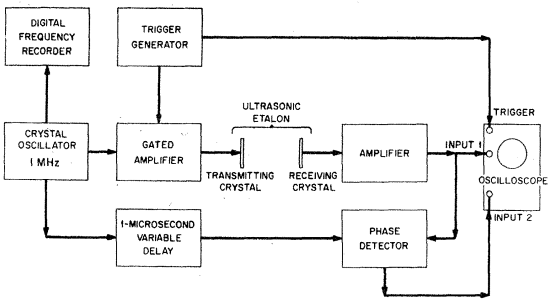


Fig. 2. Schematic diagram of electronic apparatus used for the measurement of delay.

line is not exactly a linear function of the actual delay. Such deviations from linearity were never greater than 10 nsec, or less than about 0.05% of the total delay.

The other major source of delay uncertainty was difficulty in establishing a suitable criterion for a null on the phase detector output. This was particularly difficult since the short path length and long crystal rise times forced us to make measurements during the rising transient of the received pulse. As a criterion for a null in the phase detector, we chose the situation in which the voltage at a fixed interval in time after the foot of the received pulse was zero. This point in time was chosen to be in a region in which the phase-detector output was fairly flat. By this procedure, the resultant uncertainty in null position was reduced to 20 nsec. A small amount of unfiltered carrier broadened the trace of the phase-detector output and added 10 nsec to the above uncertainty. The effect of normal electrical noise was negligible for most of the measurements, but as the critical point was approached, the signal-to-noise ratio rapidly deteriorated. For the closest measurements, the error in delay due to this source may have been as large as 250 nsec. However, this was true only for a few points taken with 1.5 Torr of the critical point.

The total transit time of the ultrasonic pulse was determined by making measurements in a region of temperature where the absolute value of the velocity is already known, and measuring delay changes relative to a reference point in this region. Such absolute measurements of sound velocity have been made in liquid helium along the vapor-pressure curve up to 4.3°K by van Itterbeek and Forrez.[20] We have matched our delay measurements to their data along the vapor-pressure curve and have thus established a fixed reference delay. Our results, therefore, reflect both the uncertainties in their data (0.1% or 20 nsec) and the uncertainties in the fit of our results to their data, approximately 30 nsec.

If we treat all of the above errors as random, the velocity uncertainty is less than 0.3% for all measurements except those very close to the critical point, where it rises to 0.6%.

Because velocity changes near the critical point are large, the maximum delay changes were much greater than one signal period $\tau_0$. Whenever the ultrasonic delay changed by an amount more than the total range of the delay line, the setting of the delay line was increased (or decreased) by $\tau_0$ to establish a new phase-detector null. To measure total delays, it is necessary to keep track of the number of cycles (integral multiples of $\tau_0$) by counting from a starting point at which the velocity is known. This is, at best, a tedious procedure, and is impossible if the sound signal is lost for any reason, which occurs when high attenuation sets in near the critical point. In order to circumvent this difficulty and to tie the data on the "gas-like" side ($P<P_c$) of the critical point to those on the "liquid-like" side ($P>P_c$), the relative delay was measured and cycles carefully counted along the trajectory shown in Fig. 3. During this circumnavigation of the critical region, the signal was never lost. The exact trajectory is unimportant as long as pressure, temperature, and relative phase are carefully measured. By this procedure, the absolute delay for data taken along any curve which intersects this trajectory can be established.

### 2.4 Pressure-Measurement System

The sample space was connected to the pressure measuring and gas-handling system through the pressure tube which ran to the top of the cryostat. A 2-liter ballast volume was attached to the pressure tube at this point to damp out pressure oscillations which often occurred in the tube in the absence of the ballast.

Pressures up to 2.5 atm were usually measured with a mercury manometer with an uncertainty of ±0.3 Torr. Some of the pressure measurements, particularly above 2.5 atm, were made with a Wallace-Tiernan differential pressure gauge calibrated against the mercury manometer below this pressure. These readings were accurate to ±1 Torr.

The hydrostatic head of helium introduces two types of errors in our measurements. The first is due to the fact that the ultrasonic measurements yield an average of the sound velocity over a range of pressures due to the finite vertical height of the measured volume, which in this case is the path length (~4 mm). At the critical density, the variation in pressure over this distance is approximately 0.02 Torr. This is an order of magnitude smaller than the uncertainty in our pressure measurements and, therefore, errors due to this effect are quite negligible.

The second type of error is caused by the fact that the pressure measured by the manometer is less than that in the sample space because of the hydrostatic head of helium in the pressure tube running up from the sample space to the mano-

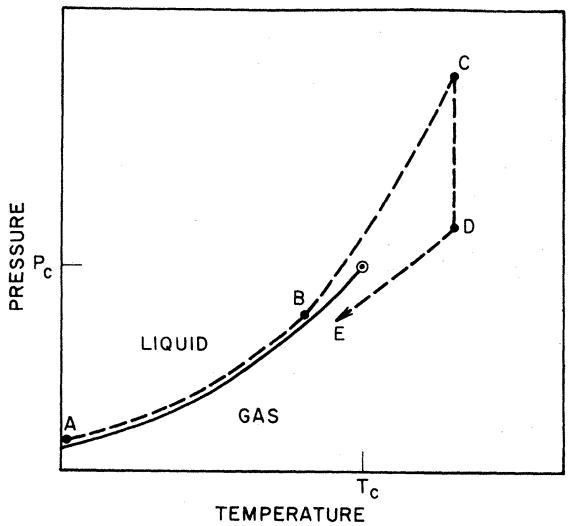


FIG. 3. Trajectory for circumnavigating the critical point. ⊙ critical point, ——: vapor pressure curve; *AB*: saturated liquid; *BC*: isochore, $\rho>\rho_c$; *CD*: isotherm, $T>T_c$; *DE*: isochore, $\rho<\rho_c$.

meter. This hydrostatic head could, in principle, be corrected for if the temperature distribution in the pressure tube and the equation of state were known. However, this information is not available. Moreover, it appears that this head varied with the level of the outer helium bath, since the pressure of the system dropped slightly (without removing any gas) whenever additional liquid helium was transferred to the bath. This variation was due to the presence of exchange gas in the vacuum space surrounding the pressure tube, which was required for the temperature controller to regulate properly. As a result, points with the same temperature and sound velocity occurred at slightly different pressures before and after transfer. Such a shift was usually less than 0.5 Torr, which corresponds to 10 cm of helium at the critical density. To minimize this effect, the helium level in the outer bath was normally maintained less than 25 cm above the can, and data near the critical point, where pressure shifts would be crucial, were taken without transferring helium between points. When such precautions were taken, points observed along an isotherm more than 24 h apart were reproduced to within 0.5 Torr.

### 2.5 Temperature Measurement and Control

A 1/10-W, 100-Ω (nominal) Allen Bradley carbon resistor, mounted on the side of the sound etalon, was used as a thermometer in this experiment. The resistor was calibrated against the saturated vapor pressure of $He^4$ using the $T^{58}$ scale.[21] The details of the experimental procedure will be discussed later. The calibration points were fitted to a four-parameter equation of the form

$$1/T = A \log R + B/(\log R + D) + C$$

by a least-squares computer program.[22] Temperatures above the highest-temperature calibration point were determined by extrapolation. Since the range of extrapolation was only 0.1 to 0.2°K and the fitting function has been found to represent the $R(T)$ relation over a wide range of temperature,[22] this procedure introduces only a small error in the determination of temperature and most of the temperature uncertainty can be ascribed to uncertainties in the calibration itself.

Since temperature errors depend on the number of calibration points, their accuracy, and the quoted temperature relative to the range of calibration temperatures, there is a different uncertainty in each run. In each of the later runs, from which most of the quantitative conclusions are drawn, more than 20 calibration points were taken between 4.1 and 5.1°K and the rms of the residuals of the four-parameter fit was less than 0.5 mdeg. Allowing a factor of 2 in the quoted uncertainty and an additional 0.5 mdeg due to extrapolation errors, the total uncertainty in these runs is probably less than ±1.5 mdeg.

## III. EXPERIMENTAL PROCEDURE

### 3.1 Calibration

At the beginning of each run the carbon resistance thermomenter was calibrated and the fixed delay to be added to relative delays was determined in the liquid along the vapor pressure curve. For each calibration point, the temperature controller was set to regulate at a fixed but unknown temperature and the ultrasonic etalon was initially covered with liquid. A sequence of data points was then taken by successively removing small amounts of gas from the sample space until several identical values of pressure and delay were observed, identifying the vapor-pressure curve. As a check, this procedure was continued until the meniscus appeared between the transducers, a situation identified by a sudden decrease in amplitude and erratic phase of the ultrasonic signal. The pressure was again read to check that it agreed with the previous values. This "pump and measure" procedure was repeated for each calibration point. As the critical point was approached, it became increasingly difficult to identify the saturation curve in this way, and reliable calibration points could not be obtained above 5.1°K.

### 3.2 Isotherms

After the above calibration was carried out, the velocity of sound along an isotherm was measured at successive pressures by removing or adding a little fluid, closing off the system, waiting for temperature and pressure equilibrium, and then measuring the pressure and phase. Whenever the experimental conditions were changed, the change in delay was followed and the cycles carefully counted. Data along isotherms were usually taken with successive points lower in pressure, because equilibrium was reached more rapidly after the removal of fluid than after its addition.

Most of the data close to the critical point were taken in two runs, during each of which measurements were made along three isotherms. Since it was possible to reproduce a temperature precisely with the automatic temperature regulator, measurements were made at all three temperatures with a given quantity of helium in the sample space; then a small quantity of gas was removed and another set of three points taken. This procedure made it possible to take data much more rapidly than would have been the case had each isotherm been followed independently, because the time required to reach equilibrium after a small temperature change was much less than that following the addition or removal of fluid. Because of this procedure, isotherms in a single run cover approximately the same range of pressure and are subject to the same systematic errors.

### 3.3 Equilibrium Precautions and Checks

One of the inherent problems of critical-point experiments is that equilibrium is difficult to establish because of long relaxation times. Several precautions were therefore taken to promote temperature and pressure equilibrium during the measurements. The inner can was con-

structed of $\frac{1}{8}$-in thick copper. The stirrer in the bottom of the inner can continuously stirred the fluid during the course of the experiments.[23] During the establishment of equilibrium, the pressure, the delay, and the error signal of the temperature controller were all observed, and measurements were made only after they were all essentially steady (usually 5–30 min). On several occasions, for conditions close to critical, we checked for drift in pressure and delay over periods of 1 to 3 h. Usually the pressure did drift slowly over this period, but the sound velocity drifted also and all data taken fell on the same experimental curve, regardless of whether the pressure was drifting up or down. Such a pressure drift could be traced to a slow warming or cooling of the pressure tube or the room-temperature plumbing and ballast volume.

We believe that these precautions were adequate to ensure equilibrium. As a further check of reproducibility, measurements were occasionally made with successive points taken both higher and lower in pressure. Usually, data taken in this way as much as a day apart were reproducible to within the normal scatter.

## IV. RESULTS

### 4.1 General

An over-all view of our results is shown in Fig. 4. The results shown in this figure will be discussed in detail below. In addition to the curves shown, measurements were made along two isobars. These measurements have previously been reported[5] and will not be discussed here.

### 4.2 Isotherms Close to the Critical Temperature

Typical results of measurements of sound velocity $u$ along isotherms passing close to the critical point are shown in Fig. 5. The observed rapid fall in velocity as the critical point is approached is in agreement with expectation. There is, in each case, a gap in pressure of width $\approx 2$ Torr over which sound-velocity measurements are impossible with the present apparatus because of high attenuation. Nevertheless, the drop outside this region is so rapid that the vanishing of $u$ at the critical point does not seem unreasonable.

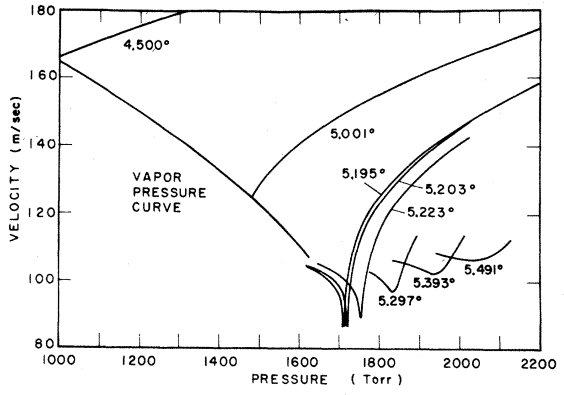


FIG. 4. Over-all view of sound velocity as a function of pressure as obtained in this experiment.

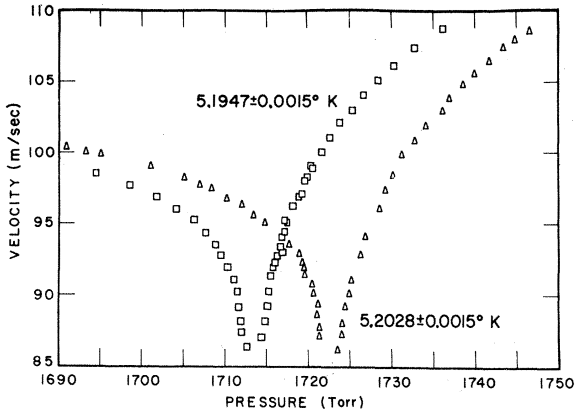


FIG. 5. Expanded plot of velocity versus pressure for two isotherms slightly above the critical temperature.

An examination of the $u(P)$ data for each isotherm shows that the shape of all the curves is quite similar, but that the origin of each curve is shifted. The degree of similarity is evident from the mathematical fits which are discussed below. If we plot in the $P$-$T$ plane the temperature of each isotherm as determined by the calibration and the pressure at the center of the "gap," we find that these points fall along the extrapolated $T^{58}$ vapor-pressure curve[21] to within the uncertainty of our measurements (Fig. 6a, b). This is consistent with data on several other substances, which indicate that specific heat and compressibility maxima occur on or near the extrapolated vapor pressure curve. If we assume this to be exactly true, this result also indicates that there are no large deviations from the shape of the vapor-pressure curve given by the $T^{58}$ scale.[21,4]

At the time these measurements were made, we assumed that the $He^4$ critical point was at the tabulated value of 1718 Torr and at 5.1994°K as given by the $T^{58}$ scale.[21] Accordingly, we concentrated our interest on isotherms near this temperature. However, subsequent measurements by Moldover and Little,[24] Roach and Douglass,[25,26] and Roach[27] have shown that the critical temperature and pressure are lower than these values. The best values for the critical parameters appear to be $P_c = 1705$ Torr and $T_c = 5.189$°K. Therefore our lowest-temperature isotherm actually is slightly above the critical temperature.

In a preliminary report,[5] we derived the adiabatic compressibility $\kappa_S = 1/\rho u^2$ using values of density $\rho$ calculated from an approximate equation of state given by Edwards and Woodbury.[28] These results suggested the existence of a logarithmic singularity in $\kappa_S$ at the critical temperature for both the liquid-like and gas-like sides, but with different slopes. However, improved estimates of density[29] subsequently contradicted this result for the low-density (gas-like) side.[16] We accordingly examined some more general functions

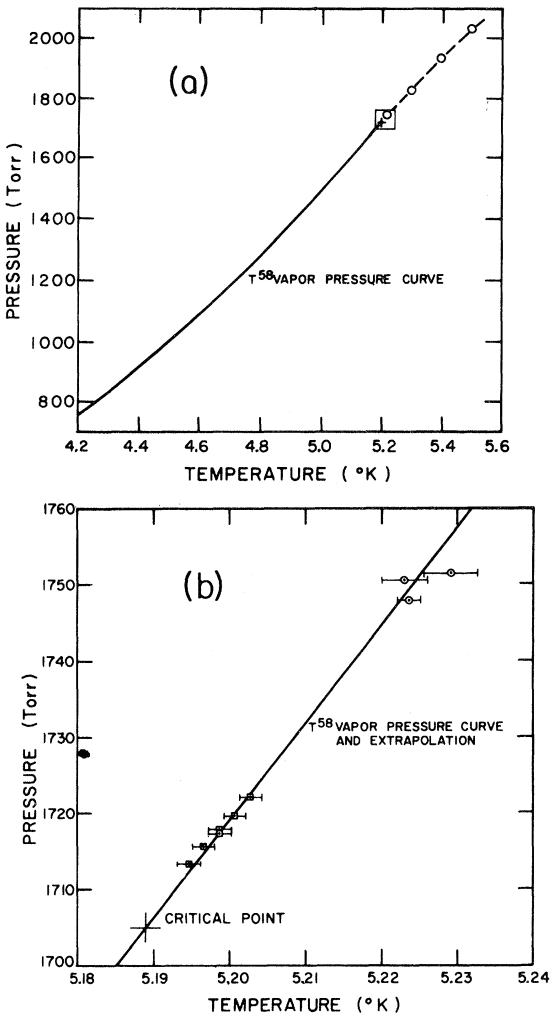


FIG. 6. (a) Locus of sound velocity minima along isotherms for $T > T_c$ in the $P$-$T$ plane; —vapor pressure curve; +critical point, ○ Present results. (b) Expanded view of the box in Fig. 6a; ⊙ locus of sound velocity minima; ⊡ locus of $P_0$'s obtained from mathematical fits to velocity data along isotherms close to the critical temperature (see text).

of the form $f(P)/u^2$, where $f(P)$ is some nonsingular function of pressure. As in Roach and Douglass's analysis of density data,[26] $f(P)$ can account for the asymmetry of the isotherms about the critical point, while the singularity is contained in the factor $u^{-2}$. It may be noted that, in principle, $f(P)$ does not affect the form of the singularity sufficiently close to the critical point. In practice, however, data must be analyzed over a range of pressures which is large enough for the form of $f(P)$ to be important. It is thus not inconsistent to search for that function which gives the experimentally observed singularity a simple mathematical form over the widest possible range.

Using the recently reported results of direct density measurements[26, 27, 30] instead of the approximate equation of state upon which we previously had to rely, we find our data to be best represented with $f(P) = \rho$. We have accordingly fitted our results to the equation

$$\rho/u^2 = -C_\pm \ln | \Delta P | + D_\pm, \tag{1}$$

where $\Delta P = [P - P_0(T)]/P_c$. Plus signs refer to values of $C$ and $D$ for $P > P_0$, and minus signs to the corresponding values for $P < P_0$.

The actual least-squares fit was carried out by independently adjusting the parameters $C_+$, $C_-$, $D_+$, $D_-$, and $P_0$ for each isotherm using an iterative procedure similar to that used by Roach and Douglass.

For each isotherm, our sound-velocity data fall on the fitted curve within the experimental uncertainty over a range of more than two orders of magnitude in $\Delta P$. In addition, $C_+ \approx C_-$, the classic form of logarithmic singularity.[31, 32] In fact, an equally good fit to the data is provided by setting $C_+ = C_-$, thus reducing the number of independently adjustable parameters from five to four. The parameters for the latter fit are given in Table I. The errors indicated are standard deviations, and do not include systematic errors. If we assume that the locus of sound-velocity minima coincides with the extrapolated vapor-pressure curve, the values of $P_0$ can provide an independent estimate of the temperature of each isotherm. These values, designated $T'$ and given in the fourth column of Table I, agree well with the measured temperatures. The results for the six isotherms given in Table I are shown in Fig. 7. Because over 500 points were taken, many have been omitted from the figure.

The logarithmic form of the divergence of $\rho/u^2$ is suggested by the scaling-law relationship derived by Helfand[33]

$$\zeta = 2\alpha/(2 + \gamma - \alpha), \tag{2}$$

where $C_v \propto \Delta\mu^{-\zeta}$, for $T = T_c$

$\mu$ = chemical potential,

$C_v \propto \Delta T^{-2}$, for $\rho = \rho_c$

$\kappa_T \propto \Delta T^{-\gamma}$, for $\rho = \rho_c$.

Since near the critical point $u^{-2} \propto C_v$ and $\Delta\mu \propto \Delta P$, we can redefine $\zeta$ in terms of the equation

$$u^{-2} \propto \Delta P^{-\zeta} \quad \text{for } T = T_c. \tag{3}$$

If $\alpha = 0$, as the specific-heat data of Moldover and Little indicate,[24] then Eq. (2) predicts $\zeta = 0$. Our data show that $u^{-2}$ is asymptotically linear in $\log \Delta P$ for $T = T_c$, which implies that $\zeta$ is indeed 0. An analogous test of this scaling law has been made in the ferromagnet, EuS, where it has been found that $C_v$ for $T = T_c$ is logarithmic in magnetic field (the analog of $\Delta\mu$).[34]

The aforementioned similarity in the shapes of the $u(p)$ isotherms is evident in Fig. 7 and in the near equality of the parameters $C$, $D_+$, and $D_-$ for each isotherm as given in Table I. Although there is a small systematic decrease in $C$ as $T$ decreases, the general shapes of the isotherms are very similar. We do not intend to imply that $u(\Delta P, \Delta T)$ goes to zero for $\Delta P = 0$, $\Delta T \neq 0$, but only that the $u(\Delta P)$ isotherms have nearly the

TABLE I. Parameters of least-squares fit to Eq. (1) for isotherms near the critical point.

| Run | $T$(°K) | $P_0$(Torr) | $T'$ (°K)[a] | $C$[b] | $D_+$[b] | $D_-$[b] |
|---|---|---|---|---|---|---|
| *A* | 5.2028 ± 0.0015 | 1722.06 ± 0.05 | 5.2025 | 1.016 ± 0.003 | 3.21 ± 0.01 | 0.65 ± 0.01 |
| *A* | 5.2008 ± 0.0015 | 1719.67 ± 0.05 | 5.2006 | 1.010 ± 0.003 | 3.22 ± 0.01 | 0.66 ± 0.01 |
| *A* | 5.1988 ± 0.0015 | 1717.24 ± 0.05 | 5.1987 | 1.001 ± 0.003 | 3.24 ± 0.01 | 0.68 ± 0.01 |
| *B* | 5.1988 ± 0.0015 | 1717.94 ± 0.03 | 5.1993 | 0.977 ± 0.003 | 3.34 ± 0.02 | 0.79 ± 0.01 |
| *B* | 5.1967 ± 0.0015 | 1715.58 ± 0.04 | 5.1974 | 0.965 ± 0.004 | 3.36 ± 0.02 | 0.83 ± 0.01 |
| *B* | 5.1947 ± 0.0015 | 1713.11 ± 0.04 | 5.1954 | 0.954 ± 0.004 | 3.39 ± 0.02 | 0.86 ± 0.02 |

[a] See text. [b] In units of $10^{-10}$ g sec$^2$ cm$^{-5}$

same shape as the critical isotherm except for values of $\Delta P$ smaller than we were able to measure. We expect that such isotherms all have a finite minimum except for the critical isotherm itself.[35]

A further implication of the similar shape of the $u(\Delta P)$ isotherms is that, for $\rho$ slightly different from $\rho_c$, the sound velocity along an isochore is only a weak function of pressure and temperature. Under the important assumption that the values of $P_0(T)$ obtained from mathematical fits to our velocity data lie on the critical isochore, the sound velocity as a function of density is shown in Fig. 8. The uncertainty in $\rho$ due to the uncertainty in pressure is shown for a few points near $\rho_c$. It is evident that over the range of our data, the sound velocity is essentially a function of density alone. However, it is obvious that this cannot be true for the critical isochore, where $u$ goes to zero at $T = T_c$.

### 4.3 Dispersion

In this experiment we used a relatively low frequency to minimize dispersion, so that our measured velocities would be close to the zero frequency (thermodynamic) limit. It is difficult to estimate whether or not we avoided significant dispersion by this choice. Several authors[11, 36 – 38] have discussed dispersion near critical points, but the predicted magnitude of dispersion is uncertain. Giterman and Kontorovich[36] have shown that the sound velocity at any nonzero frequency will not go to zero at the critical point. Significant dispersion has, in fact, been observed near the critical point in xenon at frequencies of the order of 1 MHz,[11] but dispersion was undetectable in similar measurements on carbon dioxide.[10] At much higher frequencies, however, large dispersion has been measured in $CO_2$.[39] Since our measurements were made at only one frequency, we can draw no conclusions concerning the presence or absence of significant dispersion. However, one conclusion can be drawn from the theory and experiments mentioned above. Dispersion should increase near the critical point and the velocity should decrease at lower frequencies. This would lend support to our conclusion that the thermodynamic sound velocity vanishes at the critical point and, if sig-

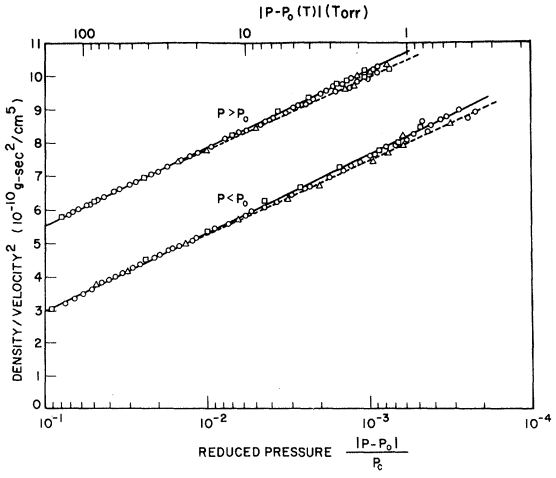


FIG. 7. The quantity $\rho/u^2$ as a function of $\ln|P-P_0|$ for isotherms close to the critical temperature. □ $T$ = 5.2028 ± 0.0015° K, —— fit to data along this isotherm; △ $T$ = 5.1947 ± 0.0015° K; 1947 fit to data along this isotherm; ○ data points along isotherms at intermediate temperatures.

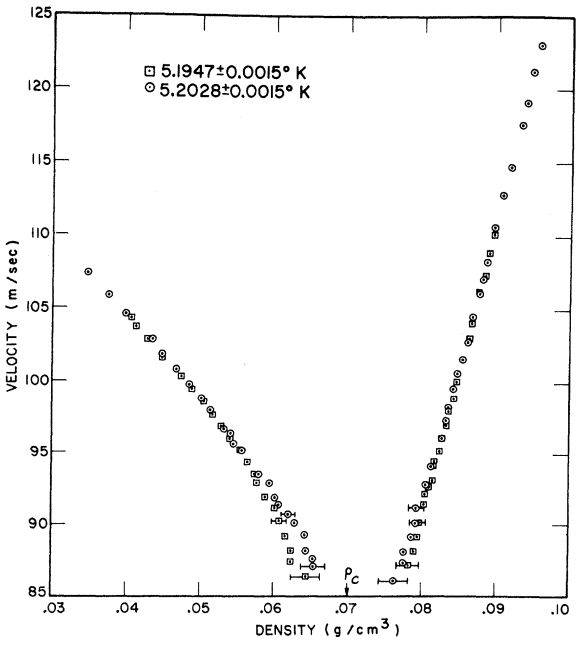


FIG. 8. Sound velocity as a function of density near the critical point.

nificant dispersion exists, the singularity in $\rho/\mu^2$ would be stronger than that which we have observed. One of us (RCW) is continuing these measurements and examining possible dispersion effects.

### 4.4 Vapor-Pressure Curve

The velocity of sound in the saturated liquid between 4 and 5.1°K is shown in Fig. 9, where it can be seen that the velocity falls rapidly as the critical point is approached. A plot of $\rho/\mu^2$ against $\ln|P_c-P|/P_c$, based on these results as well as density and velocity measurements of several investigators[20,28,40] is shown in Fig. 10, together with corresponding results for hydrogen[41] and $He^3$.[42-44] The presence of a logarithmic singularity in the $He^4$ data is clearly indicated, and the results are well represented by the equation

$$\rho/\mu^2 = C\ln|P_c-P|/P_c + D, \tag{4}$$

where $C = 1.822\times10^{-10}$ g-sec$^2$-cm$^{-5}$,

$D = 2.760\times10^{-10}$ g-sec$^2$-cm$^{-5}$,

and $P_c$ = 1705 Torr (not treated as an adjustable parameter). Hydrogen also seems to exhibit logarithmic behavior, but the $He^3$ results seem to depart slightly from such a form. Therefore, unless the latter measurements are in error, the particular form of the singularity we observe along the saturation curve may be fortuitous, and not a general property of fluids.

### 4.5 Isotherms Far Above $T_c$

Figure 4 also shows measurements along several isotherms far enough above $T_c$ for the sound velocity to be continuously observable through its minimum. The fact that the locus of these sound velocity minima in the $P, T$ plane falls approximately on the extrapolated vapor pressure curve, as shown in Fig. 6, allows us to reach some further conclusions. The following equation can be used to relate the thermodynamic sound velocity $u$ and $C_v$ near the critical point:

$$u^2 = \left(\frac{\partial P}{\partial \rho}\right)_s = \left(\frac{\partial P}{\partial \rho}\right)_t + \frac{1}{\rho^2}\left(\frac{\partial P}{\partial T}\right)_v^2 \frac{T}{C_v}. \tag{5}$$

Neglecting the first term, a plot of $u^2$ vs $T/C_v$ along the critical isochore should be a straight line of slope $[(\partial P/\partial T)_v/\rho_c]^2$. This is shown be the solid line in Fig. 11, where we have set $(\partial P/\partial T)_v$ equal to the slope of the vapor-pressure curve at $T_c$ as given by the $T^{58}$ scale. The dotted line is a correction for the nonzero value of $(\partial P/\partial \rho)_T$ calculated from the results of Roach.[27] The circles represent our values of $u_{\min}^2$ at various temperatures plotted against the specific-heat data of Moldover and Little.[24] The use of $u_{\min}$ is equivalent to the assumption that the velocity minima lie along the line $\rho=\rho_c$. The error brackets reflect uncertainties in the measured value of $C_v$ and in the temperature scale of the

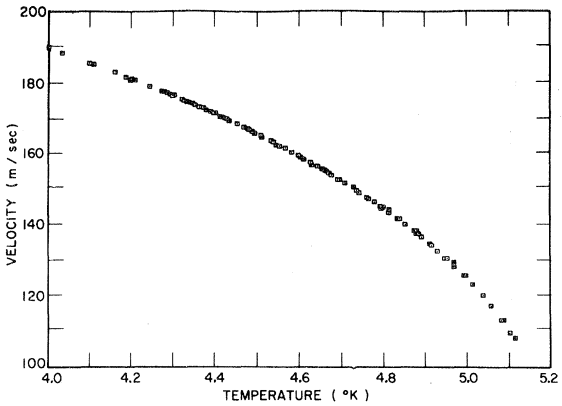


FIG. 9. Sound velocity in the saturated liquid as a function of temperature.

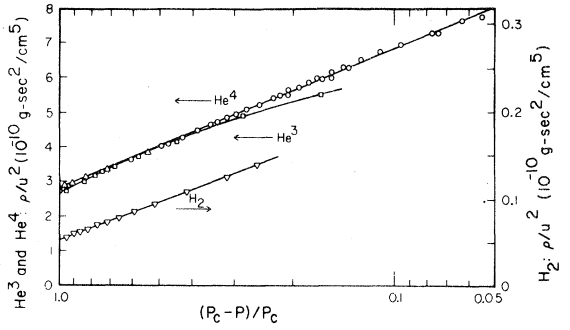


FIG. 10. $\rho/u^2$ versus $\ln(P_c-P)/P_c$ in the saturated liquid. ○ $He^4$ (this experiment and Ref. 28), △ $He^4$ (Refs. 20 and 40), □ $He^3$ (Refs. 42–44), ▽ Normal Hydrogen (Ref. 41).

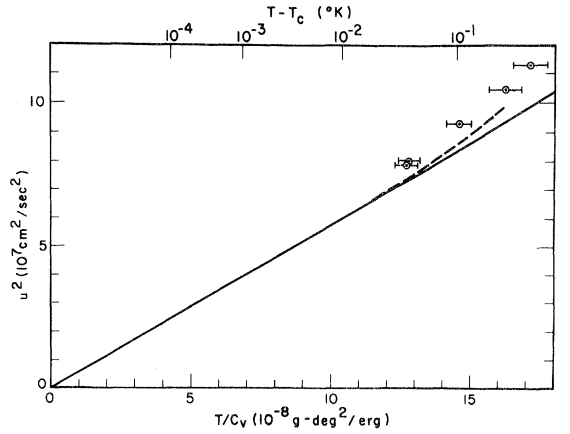


FIG. 11. Plot of $u^2_{\min}$ versus $T/C_v$ from data of Moldover and Little.[24] —— thermodynamic relationship assuming $(\partial P/\partial\rho)_T=0$, --- correction for finite value of $(\partial P/\partial\rho)_T$; ⊙ $u^2_{\min}$ (this experiment).

two experiments. There is reasonably good agreement with the prediction of Eq. (5), although all points lie 6 to 8% too high. Note that if the velocity minima did not fall exactly on the line $\rho = \rho_c$, agreement would be worse, for a smaller value of $u$ is required to fit the theoretical curve. The small systematic differences may be due to an error in our choice of $(\partial P/\partial T)_v$ or to dispersion.[45]

With the aid of the temperature scale at the top of Fig. 10, we can now estimate how low the velocity ought to fall along isotherms very close to $T_c$. The minimum velocity along an isotherm just $10^{-4}$°K above $T_c$ would be ~55 m/sec, about 2/3 of the lowest value we have observed. Thus even in an ideal experiment in which measurements could be made very close to the critical point in spite of the large attenuation there, it would hardly be possible to observe much lower values of $u$ than we have done.

### 4.6 Specific-Heat Ratio Along the Critical Isotherm and Isotherms Below $T_c$

Measurements of sound velocity in the liquid phase along isotherms at 4.5 and 5.0°K were made at pressures from the saturated vapor pressure curve up to 2200 Torr. Parts of these isotherms are shown in Fig. 4. Combining these results with the density and isothermal compressibility measurements of Edwards and Woodbury,[46] we calculate the ratio $\gamma = C_p/C_v = \kappa_T/\kappa_S$. In Fig. 12, $\gamma$ is plotted logarithmically against pressure for these two isotherms.[47] For comparison, the 4.0°K isotherm, previously calculated by Edwards and Woodbury,[46] has also been included.

Similarly, we have used the data of Roach and Douglass[26,27] to calculate $\kappa_T$ along the critical isotherm. Since $\kappa_T$ diverges like $|P - P_c|^{1-\delta}$ and $u^2$ diverges like $|P - P_c|^{-\zeta}$, where $\delta \approx 4$ and $\zeta \approx 0$, $\gamma$ should diverge to infinity at the critical point. The observed variation of $\gamma$ is indeed consistent with such a divergence, as shown in Fig. 12. We find that peak values of $\gamma$ along the critical isotherm are in excess of 100.

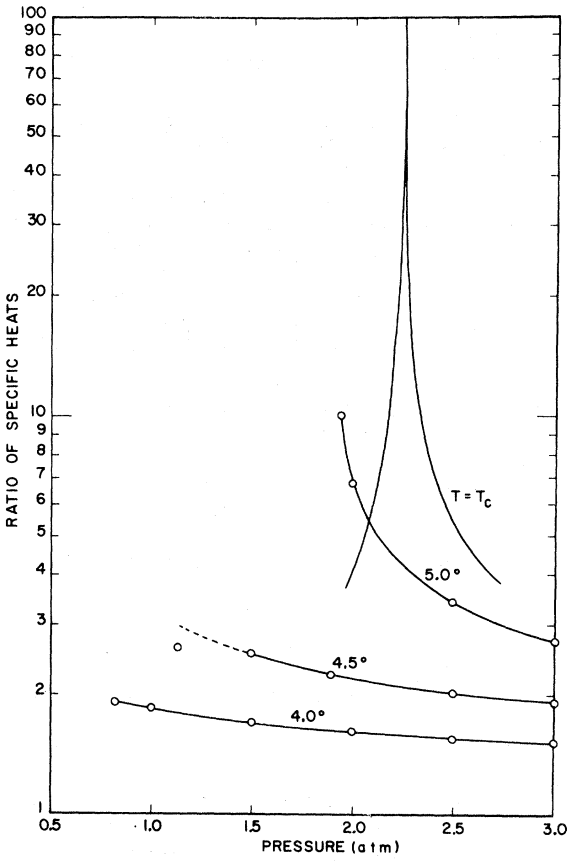


FIG. 12. Ratio of specific heats $C_p/C_v$ versus pressure along several isotherms. ○ points at which $\kappa_T$ was measured (Ref. 46). Solid curve for $T = T_c$ is calculated from the mathematical fits to the data of this experiment and the $P$-$V$-$T$ data of Ref. 26.

## ACKNOWLEDGMENTS

The authors are grateful to Laszlo Tisza for suggesting this work and for many helpful discussions during the course of the experiments, and to D. H. Douglass, Jr. and P. R. Roach for communicating their density data in advance of publication. Data reduction was greatly facilitated by the use of a computer program kindly provided by Dr. Roach.

*Supported by the U.S. Air Force Office of Scientific Research.

[1]M. I. Bagatskii, A. V. Voronel, and V. G. Gusak, Zh. Eksperim. i Teor. Fiz. 43, 728 (1962) [English transl: Soviet Physics – JETP 16, 517 (1963)].

[2]A. V. Voronel, Ya. R. Chaskin, V. A. Popov, and V. G. Simkin, Zh. Eksperim. i Teor. Fiz. 45, 828 (1963), [English transl: Soviet Physics – JETP 18, 568 (1964)].

[3]M. R. Moldover and W. A. Little in Proceedings of the Ninth International Conference on Low Temperature Physics, Columbus, Ohio, 1964; edited by J. G. Daunt *et al.* (Plenum Press, New York, 1965), p. 653.

[4]C. N. Yang and C. P. Yang, Phys. Rev. Letters 13, 303 (1964).

[5]C. E. Chase, R. C. Williamson, and L. Tisza, Phys. Rev. Letters 13, 467 (1964).

[6]C. M. Herget, J. Chem. Phys. 8, 537 (1940).

[7]J. Noury, Compt. Rend. 223, 377 (1946).

[8]W. G. Schneider, Can. J. Chem. 29, 243 (1951).

[9]N. S. Anderson and L. P. Delsasso, J. Acoust. Soc. Am. 23, 423 (1951).

[10]H. D. Parbrook and E. G. Richardson, Proc. Phys. Soc. (London) B65, 473 (1952).

[11]A. G. Chynoweth and W. G. Schneider, J. Chem. Phys. 20, 1777 (1952).
[12]H. Tielsch and H. Tanneberger, Z. Physik, 137, 256 (1954).
[13]V. F. Nozdrev, The Use of Ultrasonics in Molecular Physics, (Pergamon Press, Oxford, 1965), Chap. IV.
[14]M. A. Breazeale, J. Chem. Phys. 36, 2538 (1962).
[15]C. E. Chase and R. C. Williamson in Proceedings of the Ninth International Conference on Low Temperature Physics, Columbus, Ohio, 1964, edited by J. G. Daunt *et al.* (Plenum Press, New York, 1965), p. 657.
[16]C. E. Chase and R. C. Williamson in Critical Phenomena, Proceedings of a Conference, Washington, D. C., 1965, edited by M. S. Green and J. V. Sengers, Nat. Bur. Std. Misc. Publ. No. 273 (U. S. Government Printing Office, Washington, D. C., 1966), p. 197.
[17]C. Blake and C. E. Chase, Rev. Sci. Instr. 34, 984 (1963).
[18]C. E. Chase, Phys. Fluids 1, 193 (1958).
[19]W. M. Whitney and C. E. Chase, Phys. Rev. 158, 200 (1967).
[20]A. van Itterbeek and G. Forrez, Physica 20, 133 (1954).
[21]F. G. Brickwedde, H. van Dijk, M. Durieux, J. R. Clement, and J. K. Logan, The 1958 $He^4$ Scale of Temperatures Nat. Bur. Std. (U. S.) Monograph No. 10, (U. S. Government Printing Office, Washington, D. C., 1960).
[22]J. F. Cochran, C. A. Shiffman, and J. E. Neighbor, Rev. Sci. Instr. 37, 499 (1966).
[23]It has been suggested that stirring may disturb the long-range order which sets in at the critical point. However, our measurements are probably not close enough to the critical point for such effects to be observable.
[24]M. R. Moldover and W. A. Little, Phys. Rev. Letters 15, 54 (1965).
[25]P. R. Roach and D. H. Douglass, Jr., Phys. Rev. Letters 17, 1083 (1966).
[26]P. R. Roach and D. H. Douglass, Jr., Phys. Rev. Letters 19, 287 (1967).
[27]P. R. Roach, Phys. Rev. 170, 213 (1968).
[28]M. H. Edwards and W. C. Woodbury, Phys. Rev. 129, 1911 (1963).
[29]L. Tisza and C. E. Chase, Phys. Rev. Letters 15, 4 (1965).
[30]Values of density were calculated from one of the equations given by Roach and Douglass[26] as a fit to their data:

$$\Delta P = \mathrm{sgn}(\Delta\rho) A_{\pm} |\Delta\rho|^{\delta_{\pm}} + \frac{B\Delta T^{\gamma}\Delta\rho}{1-\frac{1}{2}\Delta\rho},$$

where

$$\Delta P = \frac{P-P_c}{P_c}, \quad \Delta T = \frac{T-T_c}{T_c}, \quad \Delta\rho = \frac{\rho-\rho_c}{\rho_c}.$$

We have assumed the following values of the critical parameters: $P_c = 1705$ Torr, $T_c = 5.189°$K, $\rho_c = 0.070$ gm/cm$^3$. The values of the other parameters in the above mathematical fit to density data are: $A_+ = 2.00$, $A_- = 1.66$, $\delta_+ = 4.00$, $\delta_- = 3.91$, $B = 5.95$, $\gamma = 1.14$.
[31]L. Onsager, Phys. Rev. 65, 117 (1944).
[32]M. J. Buckingham and W. M. Fairbank in Progress in Low Temperature Physics, edited by C. J. Gorter (North-Holland Publishing Co., Amsterdam, 1961), Vol. III, p. 86.
[33]E. Helfand, private communication referred to in Ref. 34. In this derivation and the following discussion, the variation of all nonsingular factors, in particular $\rho$, has been neglected.
[34]B. J. C. van der Hoeven, Jr., D. T. Teaney, and V. L. Moruzzi, Phys. Rev. Letters 20, 719 (1968).
[35]J. C. Wheeler and R. B. Griffiths, [Phys. Rev. 170, 249 (1968)] have shown that $C_v$ cannot be infinite along a finite line in the $P$-$T$ plane.
[36]M. Sh. Giterman and V. M. Kontorovich, Zh. Eksperim. i Teor. Fiz. 47, 2134 (1964), [English transl.: Soviet Physics – JETP 20, 1433 (1965)].
[37]R.D. Mountain, Rev. Mod. Phys. 38, 205 (1966).
[38]L. P. Kadanoff and J. Swift, Phys. Rev. 166, 89 (1968).
[39]F. W. Gammon, H. L. Swinney, and H. Z. Cummins, Phys. Rev. Letters 19, 1467 (1967).
[40]E. C. Kerr, J. Chem. Phys. 26, 511 (1957).
[41]W. van Dael, A. van Itterbeek, A. Cops, and J. Thoen, Cryogenics 5, 207 (1965).
[42]H. L. Laquer, S. G. Sydoriak, and T. R. Roberts, Phys. Rev. 113, 417 (1959).
[43]E. C. Kerr, Phys. Rev. 96, 551 (1954).
[44]G. O. Zimmerman and C. E. Chase, Phys. Rev. Letters 19, 151 (1967).
[45]Since it is likely that $(\partial^2 P/\partial T^2)_v$ diverges at the critical point,[4] there will be an anomaly in this region which makes it difficult to determine $(\partial P/\partial T)_v$ from the slope of the vapor pressure curve. We have estimated the magnitude of this correction, however, and believe it to be too small to account for the discrepancy shown in Fig. 11.
[46]M. H. Edwards and W. C. Woodbury, Can. J. Phys. 39, 1833 (1961).
[47]The point on the vapor-pressure curve at 4.5° K is probably in error. It appears that the value of $\kappa_T$ given in Ref. 46 is too low.